

# Targeted Transgene Expression in Müller Glia of Normal and Diseased Retinas Using Lentiviral Vectors

Kenneth P. Greenberg,<sup>1,2</sup> Scott F. Geller,<sup>1,2</sup> David V. Schaffer,<sup>2,3</sup> and John G. Flannery<sup>1,2</sup>

**PURPOSE.** Müller glia play crucial roles in retinal homeostasis and function. Genetic modification of Müller cells by viral gene delivery would be valuable for studies of their normal physiology and roles in retinal disease states. However, stable and efficient transgene expression in Müller cells after delivery of gene transfer vectors has remained elusive. Transcriptional and transductional targeting approaches were used to engineer recombinant HIV-1-based lentiviral (LV) vectors capable of highly efficient and sustained Müller cell transgene expression in healthy and diseased rodent retinas.

**METHODS.** Expression cassettes containing glia-specific promoters (CD44, glial fibrillary acidic protein, and vimentin) and an enhanced green fluorescent protein (eGFP) cDNA were cloned into LV backbones, which were packaged into infectious vector particles displaying either the vesicular stomatitis virus (VSV) or Ross River virus (RRV) envelope surface glycoproteins. Vectors were injected by intravitreal and subretinal approaches in wild type Sprague-Dawley (SD) and retinal degenerate S334Ter<sup>+/-</sup> transgenic rats aged 1 to 180 days. In vivo fluorescent fundus imaging and immunofluorescent confocal microscopy were used for comparison of expression efficiency, cell type specificity, and temporal expression characteristics.

**RESULTS.** The choice of viral pseudotype, regulatory promoter, and surgical delivery site each had a measurable effect on the level of eGFP transgene expression in Müller cells. The highest expression levels in SD retinas were attained with subretinal injection of VSV-G pseudotyped LV vectors containing the CD44 promoter. With these vectors, persistent eGFP expression in Müller glia was observed for more than 6 months, covering 25% to 30% of the retinal surface area after a single subretinal injection. Immunohistochemistry ( $\alpha$ -glutamine synthetase) revealed that approximately 95% of the Müller cells were transduced in the region near the injection site. Delivery of these viral vectors and subsequent Müller cell eGFP expression had no negative impact on visual function, as assessed by electroretinography (ERG).

**CONCLUSIONS.** Pseudotyped LV vectors containing glia-specific promoters efficiently transduce and direct sustained transgene expression in retinal Müller glia. Vectors of this type will be useful for experimental treatment of retinal disease, as well as

for physiological and developmental investigations of the retina. (*Invest Ophthalmol Vis Sci.* 2007;48:1844-1852) DOI: 10.1167/iovs.05-1570

Müller cells are the predominant glial cell type in the mammalian retina and serve a variety of roles vital to the health and function of surrounding retinal neurons. Müller-neuronal interactions include uptake and redistribution of K<sup>+</sup> ions released from neurons, conversion of the principal neurotransmitter glutamate into glutamine by glutamine synthetase (GS), and scavenging of free radicals released by retinal neurons via glutathione oxidation.<sup>1</sup> Also essential for neuronal energy metabolism, Müller cells release pyruvate/lactate to fuel the Krebs cycle of neighboring neurons.<sup>2,3</sup>

In addition to their known functions, Müller glia have hypothesized roles in retinal degeneration,<sup>4,5</sup> retinal neurogenesis,<sup>6</sup> and the visual cycle of cone photoreceptors.<sup>7,8</sup> Müller cells are reported to have a stereotyped activation response to photoreceptor stress caused by disease or injury,<sup>9</sup> resulting in upregulation of secreted neurotrophic factors such as basic fibroblast growth factor (bFGF) and ciliary neurotrophic factor (CNTF).<sup>5,10-12</sup> Müller cell gene transfer could allow further investigation of these novel roles, and therapies for retinal disease may result from enhancement of their endogenous neurotrophic properties.

Müller cells have a unique anatomy with processes that span the entire retinal thickness, forming the retinal margins at the inner (ILM) and outer (OLM) limiting membranes.<sup>13,14</sup> These glia are the only cell type that contact and ensheath the cell bodies and processes of every class of neuron, thereby providing both architectural and physiological support throughout the neural retina (<http://webvision.med.utah.edu/glia.html>/ developed by Helga Kolb, Eduardo Fernandez, and Ralph Nelson and provided in the public domain by the John Moran Eye Center, University of Utah, Salt Lake, City, UT). The mammalian retina contains millions of Müller glia; a ratio of 1:1 photoreceptors to Müller cells exists in the primate fovea, whereas the periphery contains 11:1.<sup>15,16</sup> These physiological and anatomic features make the Müller cell a prime target for gene transfer and therapeutic studies.

Lentiviral (LV) and adeno-associated viral (AAV) vectors have been shown to generate stable and efficient transgene expression in several classes of retinal cells in vivo, including photoreceptors, retinal pigment epithelium (RPE), and retinal ganglion cells (RGC).<sup>17-20</sup> However, viral vectors in previous studies have not yielded comparably efficient gene expression in retinal glial cells.

Directly targeting Müller cells and stably expressing a transgene by using delivery vehicles such as LV and AAV vectors has been difficult to achieve for multiple reasons. Variables including virus type, envelope glycoprotein or capsid surface proteins, and delivery approach all function to alter the cellular tropism of a given gene transfer vector. For example, investigators in previous studies have tested LV vectors displaying various non-native envelope glycoproteins and have reported these pseudotyped vectors to transduce RPE and photoreceptors preferentially.<sup>18,21</sup> AAV vectors show a strong tropism for neurons or RPE, rather than glia, when injected intraocu-

---

From the <sup>1</sup>Department of Vision Science, the <sup>2</sup>Helen Wills Neuroscience Institute, and the <sup>3</sup>Department of Chemical Engineering, University of California, Berkeley, California.

Supported by National Eye Institute Grant R01 EY13533-01, The Foundation Fighting Blindness Grant C-CA02-0701-0195, and Ruth L. Kirschstein National Research Service Award T32 EY07043-24 (KPG).

Submitted for publication December 9, 2005; revised May 26 and August 25, 2006; accepted January 24, 2007.

Disclosure: **K.P. Greenberg**, P; **S.F. Geller**, None; **D.V. Schaffer**, None; **J.G. Flannery**, P

The publication costs of this article were defrayed in part by page charge payment. This article must therefore be marked "advertisement" in accordance with 18 U.S.C. §1734 solely to indicate this fact.

Corresponding author: John G. Flannery, Helen Wills Neuroscience Institute, 112 Barker Hall, Berkeley, California 94720-3190; flannery@berkeley.edu.

larly.<sup>19,22,23</sup> Analogous targeting studies in the brain have found LV and AAV vectors to be highly neurotropic,<sup>24–26</sup> a property attributed to the envelope glycoprotein derived from the vesicular stomatitis virus (VSV-G) or the relevant AAV capsid.

Another critical factor contributing to cell-specific transgene expression is the regulatory promoter region included in the vector. In the retina, both neuronal and RPE expression have been observed when “strong” promoters such as the human cytomegalovirus (CMV), hybrid chicken  $\beta$ -actin (CAG), mouse phosphoglycerate kinase-1 (PGK-1), and spleen focus forming virus (SFFV) are delivered via LV vectors.<sup>18,27–29</sup> Previous reports of these presumably “ubiquitous” promoters indicated a lack of transgene expression in Müller cells. The restricted transgene expression observed in RPE was believed to be a result of poor binding and internalization in retinal neurons and glia, implying that VSV-G does not permit transduction of Müller cells. However, in this study, our data suggest that both VSV-G and RRV-G pseudotyped LV vectors transduce Müller cells efficiently and that transgene expression is highly dependent on the use of glial promoters.

In this article, we describe our approach to engineering a vector for the efficient and stable expression of a transgene in Müller cells *in vivo*. For maximum Müller cell specificity and expression levels, we examined several variables for their contribution to Müller cell transduction, including virus type, envelope surface glycoprotein, and delivery approach.

Furthermore, we sought to determine whether the general lack of Müller cell expression observed in previous studies was due to inefficient viral transduction or low promoter activity. To approach this question, we engineered and tested LV vectors pseudotyped with either VSV or the gliotropic Ross River virus (RRV)<sup>30,31</sup> envelope surface glycoproteins that carry eGFP expression cassettes containing various Müller cell or strong “ubiquitous” promoters. Vectors containing CD44, glial fibrillary acidic protein (GFAP), and vimentin (VIM) promoters were found to be essential for Müller cell expression, whereas strong ubiquitous promoters drove transgene expression mainly in the RPE of adult rodent retinas. Thus, viral pseudotype, promoter choice, and intraocular delivery approach are all crucial factors in achieving efficient transgene expression in Müller cells *in vivo*.

## MATERIALS AND METHODS

### LV Transfer Vector Construction

All LV transfer vectors (Fig. 1) are HIV-1-based constructs containing a CMV enhancer substituted for the U3 region of the 5' long terminal repeat (LTR) to maximize viral RNA expression during packaging.<sup>32</sup> A deletion in the U3 region of the 3' LTR renders both viral LTR pro-

motors of the integrated provirus transcriptionally silent or self-inactivating (SIN).<sup>33</sup> Promoters of interest were initially cloned into a third-generation LV backbone (pCS-CG.SP) and subsequently transferred to pFUGW (gift of David Baltimore, California Institute of Technology, Pasadena, CA) which contains the HIV-1 central polypurine tract (cPPT) and human ubiquitin-C promoter driving enhanced green fluorescent protein (eGFP) upstream of the woodchuck hepatitis virus posttranscriptional regulatory element (WPRE).<sup>34</sup> The mouse CD44 promoter (nt 185-1991 of GI 8118458) was released from CD44-pXP2<sup>35</sup> (gift of Jonathan Sleeman, University of Karlsruhe, Karlsruhe, Germany) by *Bam*HI/*Xba*I (blunted) digest and ligated in place of the ubiquitin-C promoter of a similarly digested pFUGW plasmid to construct pFmCD44GW. The mouse glial fibrillary acidic protein (GFAP) promoter (nt 70,626–68,049 of GI 27652652)<sup>36</sup> was amplified from mouse genomic DNA using the primers mGFAP/CF27 (CCGCG-GAAAGCTTAGACCCAAG), and mGFAP/CR27 (GCTAGCTTCTGC-CCTGCCTCT). The amplicon was digested with *Sac*II/*Nbe*I and ligated into a similarly digested pCS-CG.SP vector which was digested with *Sac*II (blunted)/*Age*I to release the mGFAP promoter fragment. This 2.6-kb fragment was ligated into a *Pac*I (blunted)/*Age*I digested pFUGW plasmid to construct pFmGFAPGW. The human GFAP promoter (GI 27764743)<sup>37</sup> was released from pGfa2-cLac (gift of Michael Brenner, University of Alabama, Birmingham) by *Bgl*II (blunted)/*Bam*HI digest and ligated into a *Pac*I (blunted)/*Bam*HI-digested pFUGW plasmid to construct pFhGFAPGW. The mouse VIM promoter (GI 1262330)<sup>38</sup> was amplified from mouse genomic DNA with the primers mVIM/CF6 (GAATTCGGGATCCTTGGCTGTCTTGA) and mVIM/CR6 (TCTA-GAAATCGTAGGAGCGCTGGGGTCT). The amplicon was digested with *Eco*RI/*Xba*I and ligated into a similarly digested pCS-CG.SP plasmid that was digested with *Eco*RI (blunted)/*Bam*HI. The 3.3-kb mVIM promoter fragment was ligated into a *Pac*I (blunted)/*Bam*HI digested pFUGW plasmid to construct pFmVIMGW. The hybrid CAG promoted vector contains the CMV enhancer (nt 436–954 of GI 59800) and the 1345-nt chicken  $\beta$ -actin promoter (nt 1–1345 of GI 2171233)<sup>39,40</sup> which was released from pTR-UF22WPRE (gift of Alfred Lewin, University of Florida, Gainesville, FL) by *Eco*RI digest, then blunted and ligated into a *Pac*I/*Bam*HI digested and blunted pFUGW plasmid to construct pFcAGGW. The human CMV promoter was released from pCS-CG<sup>33</sup> by *Eco*RI/*Nbe*I digest, then blunted and ligated into a *Pac*I/*Bam*HI digested and blunted pFUGW plasmid to construct pFhCMVGGW.

### Virus Production

LV vectors pseudotyped with VSV-G or RRV-G (pRRV-E2E1A, gift of David Sanders, Purdue University, West Lafayette, IN) were packaged by transient transfection (Lipofectamine 2000; Invitrogen Corp., Carlsbad, CA) of four plasmids into 293T cells as described.<sup>29</sup> High titer viral stocks were obtained after two rounds of ultracentrifugation. The vector pellet was resuspended in PBS and used immediately or flash frozen for long-term storage. Infectious titers were determined by

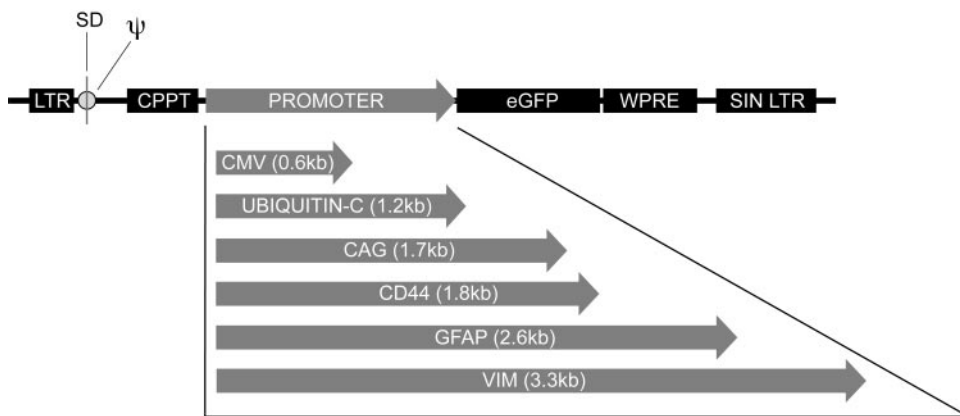


**FIGURE 1.** Schematic diagram of LV transfer vector constructs. All vectors are third-generation, HIV-1-based vectors containing the HIV-1 CPPT, promoter, eGFP cDNA, and WPRE. Promoters include human CMV, human ubiquitin-C, hybrid CMV/CAG, mouse CD44, mouse GFAP, and mouse VIM. LTR, splice donor (SD), packaging signal ( $\psi$ ), SIN LTR.

Q-PCR and flow cytometry as described<sup>29</sup> on 293T cells, as well as on cultured primary isolated rat Müller cells or a transformed rat Müller cell line (rMC-1),<sup>41</sup> generous gifts of Rong Wen (Scheie Eye Institute, University of Pennsylvania, Philadelphia, PA) and Vijay Sarthy (Northwestern University, Chicago, IL) respectively. To compare the efficiency of the promoters to be tested directly, vector stocks were diluted to contain equal titers of LV vector RNA particles/mL.

### Intraocular Injection Procedure

Sprague-Dawley (SD) or transgenic S334Ter<sup>+/-</sup> rats<sup>42</sup> were anesthetized by intraperitoneal injection of ketamine (64 mg/kg) and xylazine (7.2 mg/kg). Proparacaine hydrochloride (0.5%) was applied to the cornea, and pupils were dilated with phenylephrine (2.5%) and atropine sulfate (1%). With a medial approach, a puncture was made through the sclera near the ora serrata (~1 mm posterior to the limbus) with a sharp 30-gauge needle. Injection was via a blunt 33-gauge needle attached to a 10- $\mu$ L glass syringe (Hamilton Company, Reno, NV). Intravitreal injections were performed by inserting the blunt 33-gauge needle through the 30-gauge pilot opening and injecting 5  $\mu$ L of the vector into the vitreous. A similar procedure was used for subretinal injections. After visualization in the vitreous, the blunt needle tip was advanced through the retina into the subretinal space of the superior central retina and 3  $\mu$ L was injected into the subretinal space.

For in vivo vector comparison of the effect of surgical site, SD rats were injected either subretinally or intravitreally at P21 with VSV-CD44-GFP ( $n = 24$  eyes), VSV-GFAP-GFP ( $n = 26$  eyes), VSV-VIM-GFP ( $n = 23$  eyes), VSV-UBIQ-GFP ( $n = 14$  eyes), VSV-CMV-GFP ( $n = 22$  eyes), VSV-CAG-GFP ( $n = 25$  eyes), RRV-CD44-GFP ( $n = 12$  eyes), RRV-GFAP-GFP ( $n = 14$  eyes), RRV-VIM-GFP ( $n = 12$  eyes), RRV-UBIQ-GFP ( $n = 8$  eyes), RRV-CMV-GFP ( $n = 16$  eyes), or RRV-CAG-GFP ( $n = 16$  eyes). To examine the effect of developmental stage on LV vector transduction, we performed additional intravitreal injections on SD rats at P1 using VSV-CD44-GFP ( $n = 12$  eyes), VSV-GFAP-GFP ( $n = 11$  eyes), VSV-UBIQ-GFP ( $n = 14$  eyes), and VSV-CMV-GFP ( $n = 22$  eyes). S334Ter<sup>+/-</sup> rats were also injected at P21 and P180 with VSV-CD44-GFP ( $n = 14$  eyes), VSV-GFAP-GFP ( $n = 12$  eyes), and VSV-UBIQ-GFP ( $n = 12$  eyes) vectors. All procedures were performed in accordance with the ARVO Statement for the Use of Animals in Ophthalmic and Vision Research and were approved by the University of California, Berkeley, Committee on Animal Research.

### In Vivo eGFP Imaging

Fundus imaging was performed 2 to 180 days after injection of LV vectors with a fundus camera (Retcam II; Clarity Medical Systems Inc., Pleasanton, CA) equipped with a wide angle 130° retinopathy of prematurity (ROP) lens to monitor eGFP expression in live, anesthetized rats ( $n = 276$  eyes). Pupils were dilated for fundus imaging with phenylephrine (2.5%) and atropine sulfate (1%).

### Tissue Preparation

Retinas were detached from the RPE, fixed in 4% formaldehyde (1 hour), and embedded in molten (42°C) 5% agarose in PBS. Sections (100  $\mu$ m) were cut on a vibratome (VT1000S; Leica Microsystems GmbH, Wetzlar, Germany). For cryosections, eyes were fixed, cryo-protected in 15% followed by 30% sucrose, embedded in OCT (Tissue-Tek; Sakura Finetek USA, Inc., Torrance, CA), and sectioned at 20  $\mu$ m using a cryostat (CM1850; Leica). Immunohistochemistry was performed on VSV-CD44-GFP ( $n = 6$  eyes) and VSV-GFAP-GFP ( $n = 8$  eyes) injected retinas from SD and S334Ter<sup>+/-</sup> rats as described<sup>43</sup> using  $\alpha$ -glutamine synthetase (BD 610517, 1:1000) or  $\alpha$ -rhodopsin (Rho4D2, 1:100, gift of Robert Molday, University of British Columbia, Canada) primary antibodies, and detected using an Alexa Fluor 633-conjugated secondary antibody (A21052, 1:1000; Invitrogen-Molecular Probes, Eugene, OR). Serial confocal images were acquired on a confocal microscope (LSM-510 META 40 $\times$  Plan Neofluar 1.3 numeric aperture [NA] or 63 $\times$  Plan Apochromat 1.4 N.A. oil objectives; all from Carl Zeiss Microimaging, Inc., Thornwood, NY). Full-field 1024  $\times$  1024 optical sections were made in 0.37- $\mu$ m steps (146 sections for Fig. 5), and 3D reconstructions and movies were generated with commercial software (Imaris; Bitplane Inc., St. Paul, MN).

### Electroretinograms

One month after vector injection, SD rats ( $n = 6$ ) were dark-adapted overnight, anesthetized, and their pupils dilated. Contact lens electrodes were placed on each cornea, reference electrodes were placed subcutaneously under each eye, and a ground electrode was placed in the tail. Light stimulus was presented using a computer-controlled miniature Ganzfeld flash unit in a series of seven flashes with increasing intensity from 0.0001 to 1.0 (cd-s)/m<sup>2</sup>, and responses were recorded (Espion ERG system; Diagnosys LLC, Littleton, MA). Scotopic a-wave amplitudes were measured from baseline to the corneal negative peak and b-wave amplitudes from the corneal negative peak to the major corneal positive peak after subtracting any contributions due to oscillatory potentials. Three responses were averaged for each flash intensity. Statistical significance of amplitude differences was determined by Student's *t*-test.

### Transduction Area Measurements

The total retinal surface area expressing eGFP after subretinal injection was determined from fluorescent fundus images. Surface area measurements were based on a 3.39-mm radius eye having a total retinal surface area of 80.64 mm<sup>2</sup> (56% of the entire sphere).<sup>44</sup> Fundus images were calibrated for scale by measuring retinal vessel diameters (44.2  $\pm$  3.8  $\mu$ m) near the optic disc as seen in confocal images of flatmount retinal preparations (LSM5; Carl Zeiss Microimaging).

TABLE 1. eGFP, DNA, and RNA Titers of Concentrated LV Vectors

Transfer Vector	GFP Titer (TU/mL)	DNA Titer (TU/mL)	RNA Titer (Particles/mL)
pFUGW	1.88 $\pm$ 0.68 $\times$ 10 <sup>10</sup>	2.75 $\pm$ 0.61 $\times$ 10 <sup>10</sup>	2.68 $\pm$ 0.29 $\times$ 10 <sup>13</sup>
pFhCMVGW	4.59 $\pm$ 0.74 $\times$ 10 <sup>9</sup>	2.12 $\pm$ 0.18 $\times$ 10 <sup>10</sup>	1.10 $\pm$ 0.92 $\times$ 10 <sup>13</sup>
pFcAGGW	2.18 $\pm$ 0.52 $\times$ 10 <sup>9</sup>	1.19 $\pm$ 0.92 $\times$ 10 <sup>10</sup>	8.90 $\pm$ 0.31 $\times$ 10 <sup>12</sup>
pFmCD44GW	1.82 $\pm$ 0.34 $\times$ 10 <sup>9</sup>	2.07 $\pm$ 0.16 $\times$ 10 <sup>10</sup>	2.75 $\pm$ 0.70 $\times$ 10 <sup>13</sup>
pFmGFAPGW	4.62 $\pm$ 0.81 $\times$ 10 <sup>8</sup>	9.71 $\pm$ 0.92 $\times$ 10 <sup>9</sup>	1.72 $\pm$ 0.12 $\times$ 10 <sup>13</sup>
pFmVIMGW	2.85 $\pm$ 0.27 $\times$ 10 <sup>8</sup>	8.94 $\pm$ 0.11 $\times$ 10 <sup>9</sup>	8.80 $\pm$ 0.81 $\times$ 10 <sup>13</sup>

Comparison of VSV-G vector titers by three assays. Functional titers are expressed in transducing units/milliliter (TU/mL) on 293T cells 7 days after infection. EGFP titers were determined by flow cytometry, DNA titers (detecting integrated proviral genomes) by Q-PCR, and RNA particle titers by RT-Q-PCR.

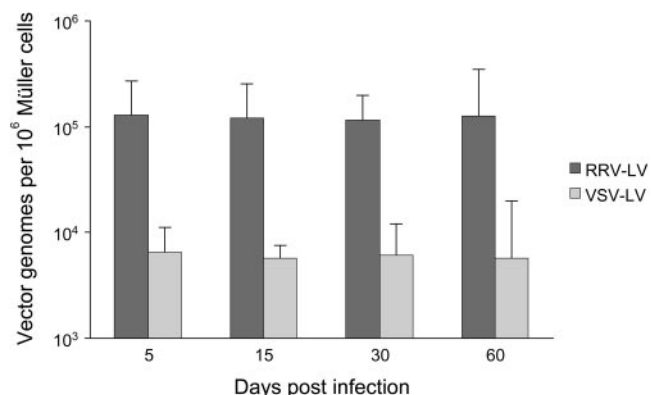


**FIGURE 2.** In vitro transduction comparison of RRV-G and VSV-G pseudotyped LV vectors. Cultured primary Müller cells ( $10^6$  cells) were infected with equivalent quantities of RRV-CMV-GFP or VSV-CMV-GFP vector particles (RNA genomes) and assayed by Q-PCR for proviral genomes 5 to 60 days later. The RRV-G vector transduced cultured Müller cells with approximately 20-fold higher efficiency than the VSV-G vector. Both vectors show stable proviral insertion for at least 60 days. Results represent the means and standard deviations of transductions performed in triplicate ( $P < 0.05$ ).

## RESULTS

### Titer Comparison of LV Vectors Using Multiple Assays

Titers of LV vectors were determined by reverse transcriptase quantitative PCR (RT-Q-PCR), quantitative PCR (Q-PCR), and flow cytometry (Table 1). These three titrating methods were used to measure RNA genomes in LV vector particles, proviral genomes in transduced cells, and eGFP expression in target cells in vitro, respectively. Functional titers obtained by flow cytometry (Poisson corrected) were approximately 1.5- to 31-fold lower than those obtained by Q-PCR detection of proviral genomes. This difference was more pronounced in vectors containing cell-specific promoters, indicating that variability in transgene expression may result in an underestimated viral titer. Q-PCR was used to avoid titer underestimation and thereby directly compare viral infectious ability regardless of promoter or transgene cassette. In addition, RT-Q-PCR was used to estimate RNA particle titers, enabling the normalization of total vector particles and the determination of infectious-to-inactive particle vector ratios which ranged from 1:500 to 1:1800.

### In Vitro Vector Characterization on Cultured Müller Cells

LV backbone constructs (Fig. 1) were packaged into infectious particles and initially characterized by infecting cultures of primary isolated rat Müller cells or a transformed rat Müller cell line (rMC-1). Viral transduction efficiency of VSV-G and RRV-G vectors was quantified via Q-PCR<sup>29,45</sup> after infection of primary Müller cells with equivalent quantities of viral RNA particles. This analysis revealed that RRV-G pseudotyped vectors exhibited a 20-fold higher transduction efficiency than VSV-G vectors in vitro (Fig. 2). In addition, eGFP expression was observed in both the primary Müller and rMC-1 cell lines after infection with RRV-G pseudotyped vectors containing the CAG, VIM, and GFAP promoters (Fig. 3).

### In Vivo CD44, GFAP, and VIM Promoter-Driven eGFP Expression

LV vectors pseudotyped with VSV-G and RRV-G were tested in vitro and in vivo. Although the RRV glycoprotein permitted

higher Müller cell transduction levels than the VSV glycoprotein during in vitro testing on primary Müller cell cultures (Fig. 2), VSV-G pseudotyped vectors consistently yielded higher Müller cell transgene expression when tested in vivo. VSV-G vectors were therefore chosen for subsequent in vivo experiments and Müller cell promoter analysis.

After subretinal injection of VSV-G vectors with CD44, GFAP, and VIM promoters, eGFP was consistently seen by fundus imaging (Figs. 4A-C). Of these glial promoters, overall fluorescence intensity appeared highest with the CD44 promoter, followed by GFAP, and finally VIM promoter vectors (Figs. 4A-C). The VSV-CMV vector drove relatively strong expression (Fig. 4D); however, histologic examination revealed CMV-GFP expression was restricted to the RPE and was not observed in Müller cells (described later). EGFP was observed over a 6-month period after subretinal injection of VSV-G pseudotyped CD44, GFAP, VIM, and CMV promoted vectors, suggesting persistent transgene expression and stable proviral integration (Figs. 4A-D). No eGFP expression was observed with intravitreal injection of LV vectors (Fig. 4E).

Confocal microscopy strikingly revealed that Müller cells were transduced with high efficiency with subretinal injection of the VSV-CD44 vector (Fig. 5 and Movie 1, online at <http://www.iovs.org/cgi/content/full/48/4/1844/DC1>). This significant finding contrasts with previous reports that indicated extremely low or no Müller cell expression with VSV-G pseudotyped LV vectors.<sup>18,21,23</sup> VSV-CD44 vector injected retinas exhibited eGFP expression in Müller cell processes spanning the entire retinal thickness (Fig. 6A). Detailed Müller cell anatomy including processes enveloping photoreceptor cell bodies (Fig. 6B) and the complex fiber basket matrix at the OLM were observed en face (Fig. 6C). To provide further

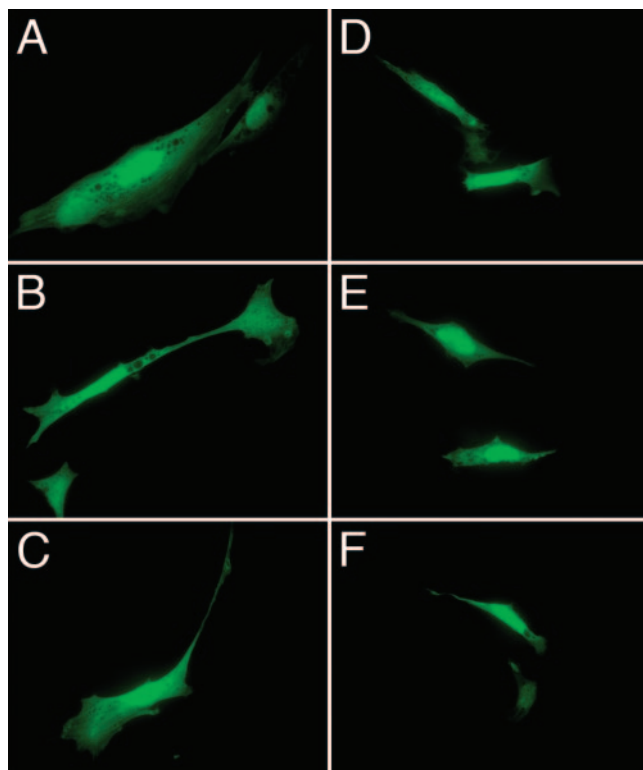


**FIGURE 3.** Cultured rat Müller cells express eGFP delivered by RRV-G pseudotyped LV vectors. (A-C) Primary Müller cells and (D-F) rMC-1 cells expressing eGFP. (A, D) RRV-CAG-GFP, (B, E) RRV-VIM-GFP, and (C, F) RRV-GFAP-GFP. All three promoters drive expression in cultured Müller cells.

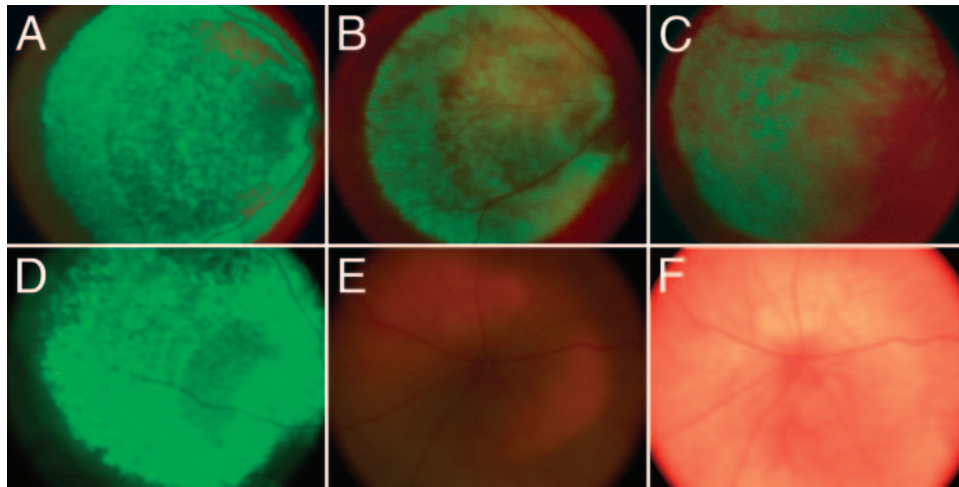


**FIGURE 4.** Subretinal injection of VSV-G pseudotyped LV vectors drives stable eGFP expression in vivo. Fluorescent fundus views of SD rat retinas injected subretinally with (A) VSV-CD44-GFP, (B) VSV-GFAP-GFP, (C) VSV-VIM-GFP, (D) VSV-CMV-GFP. (E) No eGFP expression is observed after intravitreal injection of VSV-CD44-GFP vector. (F) Bright-field view of the same retina as shown in (E). All LV vector stocks were diluted in PBS to contain  $3.3 \times 10^{10}$  viral RNA particles in a  $3 \mu\text{L}$  subretinal injection (A–D). For (E–F),  $1.4 \times 10^{11}$  RNA particles were injected intravitreally in  $5 \mu\text{L}$ . All retinas shown were injected at P21 and imaged at P200. Fundus imaging was performed at equivalent UV excitation intensity levels, to estimate relative fluorescence levels among these promoters.

confirmation, we immunostained eGFP-positive sections with a Müller cell-specific antibody to glutamine synthetase (GS), which exhibited colocalization with LV-mediated eGFP expression (Figs. 6D–F).

To explore the capacity of these vectors to deliver transgenes to Müller cells in the diseased retina, we next tested

them in the degenerating  $S334\text{Ter}^{+/-}$  transgenic rat. After subretinal injection of the VSV-GFAP vector in the  $S334\text{Ter}^{+/-}$  retina, eGFP-positive Müller cells were seen to extend beyond the OLM and invade the subretinal space of rhodopsin-stained photoreceptor outer segments (Figs. 6G–I). Obvious signs of reactive gliosis and glial scar formation were observed in eGFP-

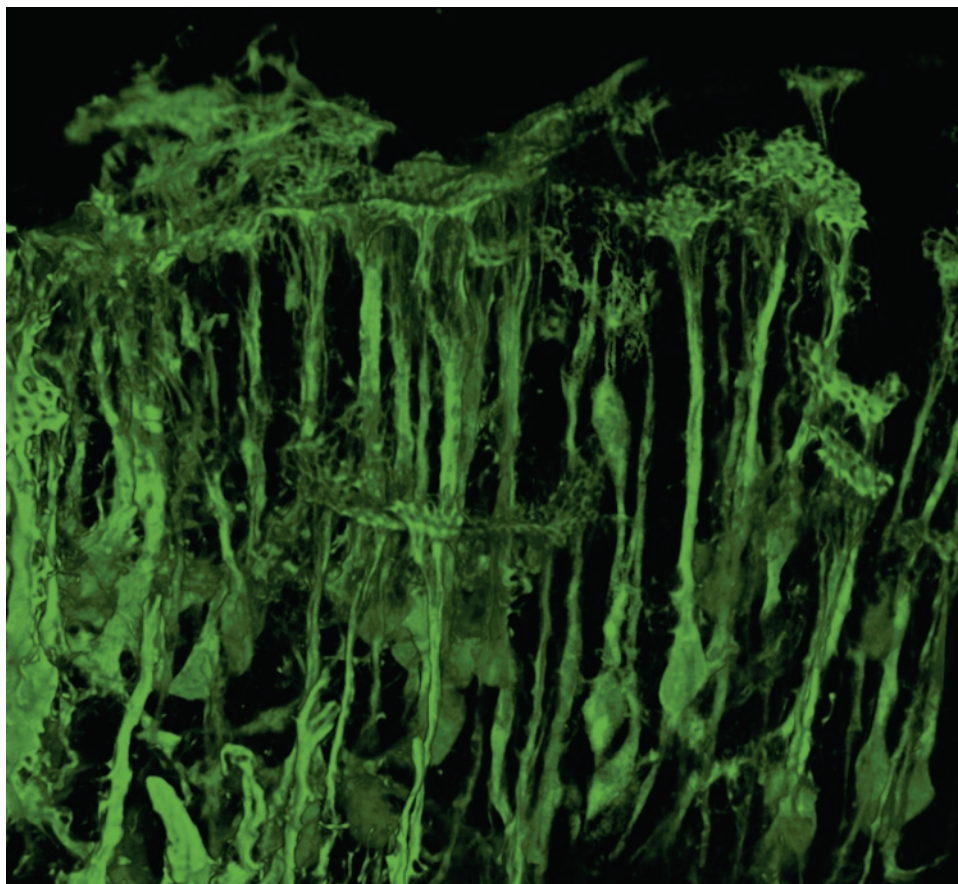
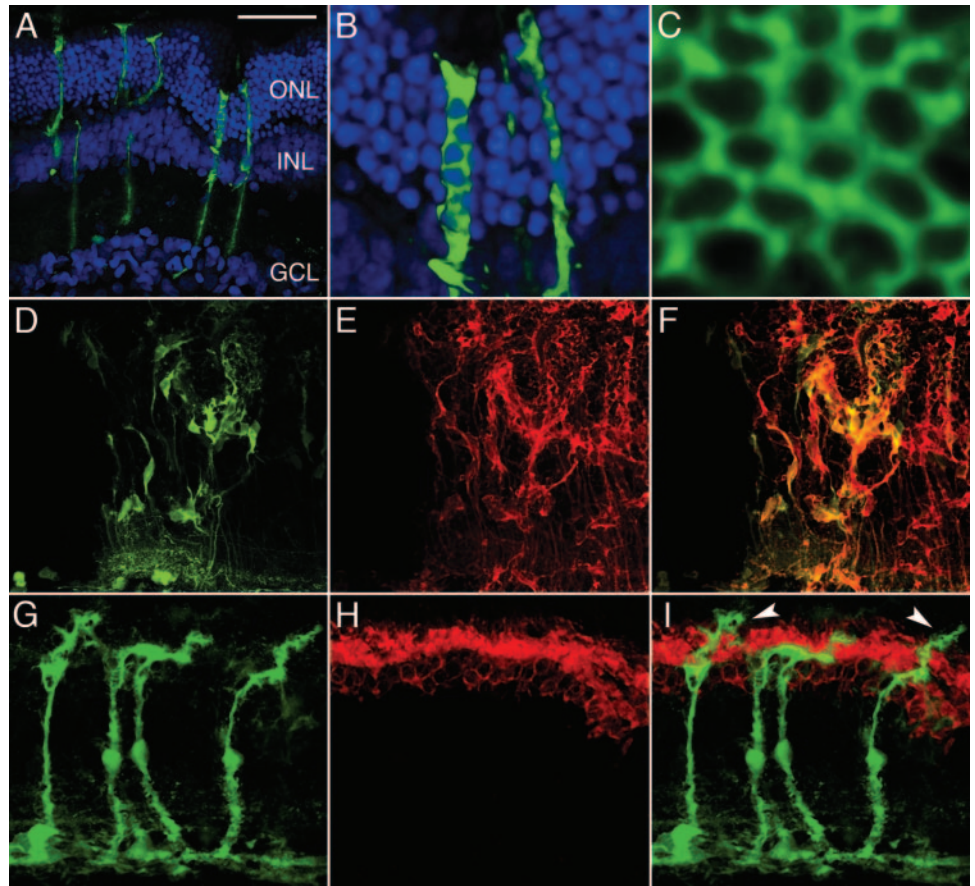


**FIGURE 5.** High Müller cell transduction efficiency and detailed anatomy are observed after LV vector mediated eGFP delivery. Serial confocal image reconstruction of SD rat retina ( $100\text{-}\mu\text{m}$  thick agarose section) 10 days after subretinal injection of VSV-CD44-GFP LV vector. OLM and branched fiber basket matrix of eGFP-positive Müller cells are seen at top of image.

**FIGURE 6.** LV vector delivered eGFP expression in healthy and diseased retinas. One month after VSV-CD44-GFP vector injection at P21 (A) eGFP-positive Müller cells are observed spanning the entire thickness of SD rat retina (A–F) far from the injection site (ONL curvature is a tissue processing artifact). (B) Müller cell processes surround DAPI-stained photoreceptor nuclei (blue). (C) High-magnification en face view of Müller cell fiber basket matrix at the OLM. (D) eGFP positive, (E) glutamine synthetase-stained (red), and (F) merged Müller cells are disorganized, most likely as a result of the subretinal injection procedure. Two months after VSV-GFAP-GFP vector injection at P21, (G) eGFP-positive Müller cells were observed in the diseased S334Ter<sup>±</sup> retina (G–I). (H) Photoreceptor outer segments were stained with a rhodopsin antibody (red). (I) The merged image indicates the relationship between the Müller cells and the photoreceptor outer segments; Müller cell apical processes (arrowheads) have emerged beyond the OLM and into the subretinal space. DAPI (blue) was used to counterstain nuclei in (A–B). Scale bar, 50  $\mu$ m.



positive Müller cells of degenerating S334Ter<sup>+/-</sup> retinas 2 months after injection (Figs. 7A–C). S334Ter<sup>+/-</sup> retinas injected with vectors containing the GFAP promoter exhibited the highest eGFP expression levels relative to vectors containing the CD44 or VIM promoters. Increased GFAP promoter activation in S334Ter<sup>+/-</sup> retinas therefore makes the VSV-GFAP vector the preferred choice for these diseased retinas. Overall, Müller cell transduction levels appeared higher in the degenerate S334Ter<sup>+/-</sup> retinas when compared to wild-type SD retinas, regardless of vector pseudotype or promoter. This observation was most pronounced when injections were performed in older (P180) diseased retinas in a highly “reactive” state (Fig. 7).

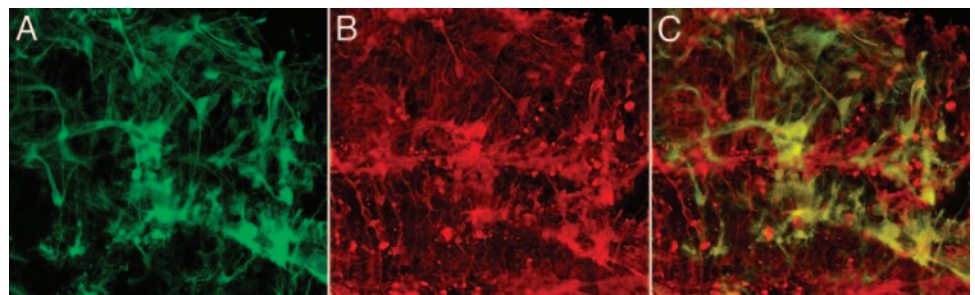
Although targeted eGFP expression was seen in Müller cells in SD and S334Ter<sup>+/-</sup> retinas injected with VSV-CD44, VSV-GFAP, and VSV-VIM vectors, “leaky” expression was observed in adjacent RPE cells (data not shown). In contrast to these glial promoters, LV vectors containing the CMV and ubiquitin promoters drove eGFP expression solely in the RPE when injected subretinally in adult SD rats (Fig. 8). We have previously shown

photoreceptor transduction when VSV-CMV vectors were injected before P7<sup>29</sup>; however, eGFP expression in the adult neural retina was only observed at the injection site. In the present study, both VSV-G and RRV-G pseudotyped vectors containing ubiquitous promoters yielded RPE-restricted eGFP expression in adult retinas (Fig. 8).

### High-Efficiency LV Vector Transduction of Müller Cells

Müller cells are transduced with high efficiency in the area of the subretinal detachment when viewed in serial confocal section as in Figure 5. Quantitative calculations of Müller cell density indicate that the rat retina contains 12,000 Müller cells/mm<sup>2</sup>.<sup>16</sup> Therefore, nearly 1 million Müller cells exist in an entire rat retina having a total surface area of 81 mm<sup>2</sup>.<sup>44</sup> We calculated the retinal surface area transduced after a 3- $\mu$ L subretinal injection of vector based on in vivo fluorescent fundus images (Retcam II; Clarity Medical Systems Inc.). Approximately 29 mm<sup>2</sup>, or 36% of the entire rat retina is viewable

**FIGURE 7.** Müller cells in the diseased retina. Reactive gliosis caused by combined injury of the subretinal injection procedure and genetic retinal degeneration resulted in glial scar formation seen in a cross-section of S334Ter<sup>+/-</sup> rat retina injected with VSV-GFAP-GFP vector. (A) eGFP, (B)  $\alpha$ -glutamine synthetase, (C) merged image. Retina injected at P180 and imaged at P242.



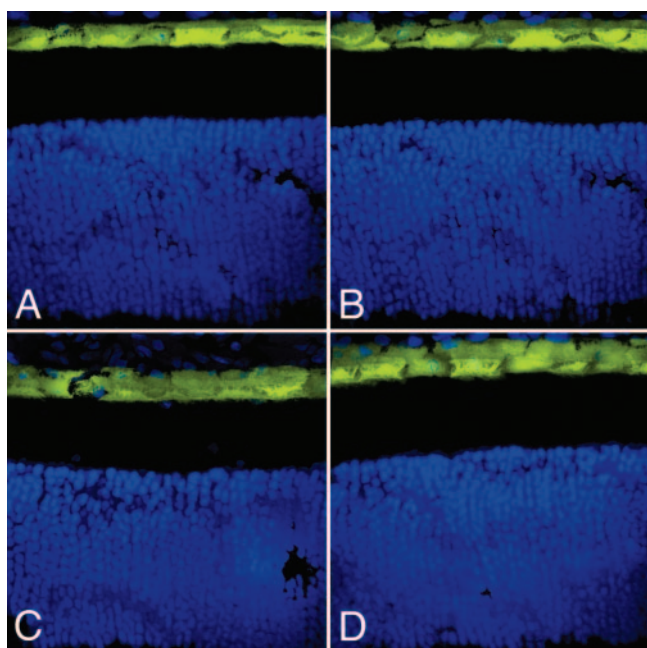


**FIGURE 8.** The CMV and ubiquitin promoters drive eGFP expression in the RPE when delivered by VSV or RRV pseudotyped vectors. (A) VSV-CMV, (B) VSV-ubiquitin, (C) RRV-CMV, and (D) RRV-ubiquitin vectors drive eGFP expression restricted to the RPE when injected subretinally. SD rat retinas were injected at P21 and imaged at P30. DAPI (blue) was used to counterstain the nuclei.

in a single fundus image. We conservatively estimate that a 3- $\mu$ L subretinal injection results in the transduction of 20 mm<sup>2</sup> (25% of the entire retina) or 68% of the entire field. From these calculations, a single injection can transduce approximately 228,000 Müller cells, based on a density of 12,000 Müller cells/mm<sup>2</sup> and 95% transduction efficiency. This population of transduced Müller cells provides physiological support for approximately 7.1 million retinal neurons or 5.7 million photoreceptor cells in the rat retina.<sup>16</sup>

### Effect of LV Vector Injection on ERG

We sought to determine whether subretinal injection of LV vectors delivering eGFP to Müller cells affects retinal function as assessed by ERG. The “Müller cell hypothesis” suggests that the ERG b-wave results from changes in Müller cell membrane potential arising from light-induced fluctuations of extracellular potassium concentration due to depolarizing retinal neurons.<sup>46</sup> However, recent studies in which barium ions were used to block the potassium permeability of Müller cells suggest that ON-center bipolar cells generate the b-wave without contribution by Müller cells.<sup>47</sup> We evaluated scotopic ERG responses to increasing intensities of light from dark-adapted rats injected subretinally with LV vectors or PBS (Fig. 9). Data obtained from SD rats ( $n = 6$ ) suggest that Müller cell expression of eGFP does not significantly affect the ERG.

### DISCUSSION

Glial cells in the central nervous system (CNS) have remained difficult targets for gene delivery studies despite empiric analysis of several combinations of parent virus, envelope glycoprotein or capsid, promoter, and delivery method. Although the exact mechanism underlying glial or neuronal tropism is not entirely understood, cell surface receptor profile, promoter methylation, and cellular machinery for processing foreign DNA all may play im-

portant roles. Although significant research has failed to unequivocally identify the surface receptors required for attachment and internalization of VSV-G and RRV-G pseudotyped viruses, both glycoproteins have been shown to mediate viral entry by clathrin-dependent endocytosis.<sup>48–50</sup> Therefore, we are uncertain of the receptors used by these LV vectors for Müller cell transduction. Our *in vitro* data indicate that RRV-G pseudotyped vectors transduced Müller cells with higher efficiency than did VSV-G vectors (Fig. 2); however, *in vivo* tests did not show the RRV-G envelope to provide a clear advantage in either efficiency or tropism. Furthermore, overall packaging efficiency of RRV-G pseudotyped vectors was significantly lower than VSV-G, leading to lower titers.

LV vectors were chosen for this study because of their large transgene capacity, rapid onset of expression, and robust long-term expression profile. Previous reports using adenoviral (Ad) vectors have demonstrated Müller cell transduction,<sup>51</sup> but Ad vectors exhibit transient expression (4 weeks), restricting their use in long-term therapeutic strategies. Furthermore, Ad vectors evoke an immune response when delivered to the retina, necessitating the use of immunosuppression.<sup>51,52</sup> Unlike LV and Ad vectors, AAV vectors transduce retinal neurons with high efficiency,<sup>17,20</sup> though their Müller cell transduction efficiency is extremely low.<sup>53</sup> In addition, AAV transgene capacity is ~4.7 kb, limiting the use of prototypical full-length promoters and large cDNAs.

Promoters for this study were selected based on their native gene expression levels and retinal cell-type specificity. Immunohistochemistry on human and rodent retinas has revealed that CD44 is localized to Müller cell apical microvilli, projecting above the adherens junctions of the OLM and into the interphotoreceptor matrix (IPM) of the subretinal space.<sup>54</sup> We reasoned that the CD44 promoter, previously uncharacterized in the retina, could confer specific glial expression, because this protein has not been detected in differentiating or mature neurons in the retina or brain.<sup>55</sup> CD44 is a widely expressed transmembrane glycoprotein and cell surface receptor for hyaluronic acid and is also thought to mediate cell migration, retinal adhesion, tissue differentiation, and cellular responses to trauma and disease.<sup>56</sup> GFAP, a major component of glial filaments in Müller cells, astrocytes, and microglia, is a type III intermediate filament protein that is dramatically upregulated in response to injury or stress.<sup>57</sup> We tested LV vectors containing the human (2.2 kb) and mouse (2.6 kb) GFAP promoters, both of which have been characterized in some detail.<sup>37,58</sup> The mouse promoter consistently provided higher protein expression levels in rodent Müller cells and was used exclusively in this study. VIM is an intermediate filament protein expressed in Müller cells, reactive astrocytes, and RPE.<sup>59</sup> VIM, like GFAP, is highly upregulated in response to injury or stress, though its role in the healthy retina is unclear. Studies using VIM knock-

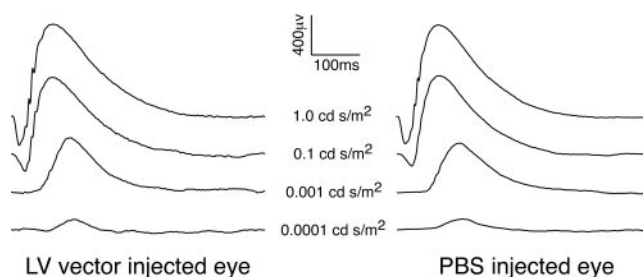


**FIGURE 9.** Scotopic ERG recordings after LV vector injection. Example of dark-adapted ERG traces from VSV-CD44-GFP vector and PBS-injected eyes recorded 1 month after injection of P21 rats. No significant difference in b-wave amplitude was observed between vector injected and PBS control eyes.

out mice exposed to mechanical challenge show VIM is important for maintaining the mechanical integrity of Müller cell endfeet and inner retinal layers.<sup>60</sup> VIM promoter activity has not been fully characterized in the retina; however, a highly conserved 188-bp fragment of the proximal VIM promoter was reportedly sufficient for effective transcription in myeloid leukemia cells.<sup>38</sup>

Both intravitreal and subretinal injection delivery approaches were evaluated with these LV vectors. Regardless of promoter, pseudotype, or animal age at injection (P1-P180), the subretinal approach consistently yielded eGFP expression (Figs. 4A-D), whereas the intravitreal approach yielded none (Fig 4E), in agreement with previous reports.<sup>18,23</sup> The nature of the barriers to LV vector retinal transduction at the vitreal surface are not well understood. Potential barriers include proteins known to bind and inactivate retroviral vectors,<sup>61</sup> a physically dense collagen fibril network, a polarized receptor profile on the Müller cell surface, the relative instability (compared to AAV) and large particle size (80-100 nm) of LV vectors. AAV2 vectors clearly have the ability to traverse the ILM and efficiently transduce RGCs when injected intravitreally.<sup>19,20</sup> For comparison, we also tested AAV2 vectors containing the CD44-GFP expression cassette and observed no expression in Müller cells after intravitreal or subretinal injection in SD rats. However, a subset of RGCs were observed to be eGFP positive after intravitreal injection of AAV2-CD44-GFP (data not shown), in agreement with the reported neurotropism of AAV2 vectors.<sup>26,29</sup>

One natural function of Müller cells may be to directly protect photoreceptors from apoptosis during retinal stress through neurotrophin modulation and secretion.<sup>4,5,62</sup> Presumably, healthy Müller cells could be modified to secrete universal neuroprotective factors continuously (i.e., GDNF, bFGF),<sup>20,51,63-65</sup> to treat blinding diseases such as age-related macular degeneration (AMD), glaucoma, and retinitis pigmentosa (RP). Expression of these neuroprotective factors under the control of stress-inducible promoter elements such as GFAP, VIM, and CD44, taken from genes that are dramatically upregulated during injury or disease,<sup>55,57,66</sup> could allow neurotrophin levels to be endogenously modulated as needed. The human retina contains 8,500 to 11,000 Müller cells/mm<sup>2</sup>, or an average of 10.7 million Müller cells.<sup>16</sup> Estimates extrapolated from the rat to the human retina (considering species and size differences) indicate that a 50- $\mu$ L subretinal injection of vector could transduce approximately 3.3 million Müller cells or 30% of the entire retina. This large population of Müller cells provides support for nearly 50 million retinal neurons or 36 million photoreceptors.<sup>16</sup>

In summary, we have demonstrated that delivery of LV vectors containing glia-specific promoters by subretinal injection allows high-level transgene expression in Müller cells. We have explored targeting these essential glial cells through exchange of transcriptional regulatory elements, pseudotyping with non-native viral envelope surface glycoproteins, and two surgical delivery approaches. Future studies will be designed to use these vectors to study retinal disease and normal retinal physiology.

### Acknowledgments

The authors thank Julie Yu, Joshua Leonard, James Koerber, William Hauswirth and Vince Chiodo for advice regarding LV and AAV vector production and Daniel Paskowitz for critical comments on the manuscript.

### References

1. Reichenbach A, Robinson SR. The involvement of Müller cells in the outer retina. In: Djamgoz MBA, Archer SN, Vallergera S, eds.

- Neurobiology and Clinical Aspects of the Outer Retina*. London: Chapman & Hall; 1995;395-416.
- Bringmann A, Skatchkov SN, Pannicke T, et al. Müller glial cells in anuran retina. *Microsc Res Tech*. 2000;50:384-393.
  - Newman E, Reichenbach A. The Müller cell: a functional element of the retina. *Trends Neurosci*. 1996;19:307-312.
  - Zack DJ. Neurotrophic rescue of photoreceptors: are Müller cells the mediators of survival. *Neuron*. 2000;26:285-286.
  - Harada T, Harada C, Nakayama N, et al. Modification of glial-neuronal cell interactions prevents photoreceptor apoptosis during light-induced retinal degeneration. *Neuron*. 2000;26:533-541.
  - Fischer AJ, Reh TA. Potential of Müller glia to become neurogenic retinal progenitor cells. *Glia*. 2003;43:70-76.
  - Mata NL, Radu RA, Clemmons RC, Travis GH. Isomerization and oxidation of vitamin A in cone-dominant retinas: a novel pathway for visual-pigment regeneration in daylight. *Neuron*. 2002;36:69-80.
  - Mata NL, Ruiz A, Radu RA, Bui TV, Travis GH. Chicken retinas contain a retinoid isomerase activity that catalyzes the direct conversion of all-trans-retinol to 11-cis-retinol. *Biochemistry*. 2005;44:11715-11721.
  - Rattner A, Nathans J. The genomic response to retinal disease and injury: evidence for endothelin signaling from photoreceptors to glia. *J Neurosci*. 2005;25:4540-4549.
  - Cao W, Li F, Steinberg RH, LaVail MM. Development of normal and injury-induced gene expression of aFGF, bFGF, CNTF, BDNF, GFAP and IGF-I in the rat retina. *Exp Eye Res*. 2001;72:591-604.
  - Harada T, Harada C, Kohsaka S, et al. Microglia-Müller glia cell interactions control neurotrophic factor production during light-induced retinal degeneration. *J Neurosci*. 2002;22:9228-9236.
  - Wen R, Cheng T, Song Y, et al. Continuous exposure to bright light upregulates bFGF and CNTF expression in the rat retina. *Curr Eye Res*. 1998;17:494-500.
  - Müller H. Zur Histologie der Netzhaut. *Z Wiss Zool*. 1851;234-237.
  - Cajal S. *The Structure of the Retina*. Translated by Thorpe SA, Glickstein M. Springfield, IL: Thomas; 1972.
  - Burriss C, Klug K, Ngo IT, Sterling P, Schein S. How Müller glial cells in macaque fovea coat and isolate the synaptic terminals of cone photoreceptors. *J Comp Neurol*. 2002;453:100-111.
  - Chao TI, Grosche J, Friedrich KJ, et al. Comparative studies on mammalian Müller (retinal glial) cells. *J Neurocytol*. 1997;26:439-454.
  - Flannery JG, Zolotukhin S, Vaquero MI, et al. Efficient photoreceptor-targeted gene expression in vivo by recombinant adeno-associated virus. *Proc Natl Acad Sci USA*. 1997;94:6916-6921.
  - Duisit G, Conrath H, Saleun S, et al. Five recombinant simian immunodeficiency virus pseudotypes lead to exclusive transduction of retinal pigmented epithelium in rat. *Mol Ther*. 2002;6:446-454.
  - Martin KR, Quigley HA, Zack DJ, et al. Gene therapy with brain-derived neurotrophic factor as a protection: retinal ganglion cells in a rat glaucoma model. *Invest Ophthalmol Vis Sci*. 2003;44:4357-4365.
  - Malik JM, Shevtsova Z, Bahr M, Kugler S. Long-term in vivo inhibition of CNS neurodegeneration by Bcl-XL gene transfer. *Mol Ther*. 2005;11:373-381.
  - Miyoshi H, Takahashi M, Gage FH, Verma IM. Stable and efficient gene transfer into the retina using an HIV-based lentiviral vector. *Proc Natl Acad Sci USA*. 1997;94:10319-10323.
  - Yang GS, Schmidt M, Yan Z, et al. Virus-mediated transduction of murine retina with adeno-associated virus: effects of viral capsid and genome size. *J Virol*. 2002;76:7651-7660.
  - Auricchio A, Kobinger G, Anand V, et al. Exchange of surface proteins impacts on viral vector cellular specificity and transduction characteristics: the retina as a model. *Hum Mol Genet*. 2001;10:3075-3081.
  - Blomer U, Naldini L, Kafri T, et al. Highly efficient and sustained gene transfer in adult neurons with a lentivirus vector. *J Virol*. 1997;71:6641-6649.
  - Kordower JH, Bloch J, Ma SY, et al. Lentiviral gene transfer to the nonhuman primate brain. *Exp Neurol*. 1999;160:1-16.



26. Burger C, Gorbatyuk OS, Velardo MJ, et al. Recombinant AAV viral vectors pseudotyped with viral capsids from serotypes 1, 2, and 5 display differential efficiency and cell tropism after delivery to different regions of the central nervous system. *Mol Ther.* 2004;10:302-317.
27. Tschernutter M, Schlichtenbrede FC, Howe S, et al. Long-term preservation of retinal function in the RCS rat model of retinitis pigmentosa following lentivirus-mediated gene therapy. *Gene Ther.* 2005;12:694-701.
28. Kostic C, Chiodini F, Salmon P, et al. Activity analysis of house-keeping promoters using self-inactivating lentiviral vector delivery into the mouse retina. *Gene Ther.* 2003;10:818-821.
29. Greenberg KP, Lee ES, Schaffer DV, Flannery JG. Gene delivery to the retina using lentiviral vectors. *Adv Exp Med Biol.* 2006;572:255-266.
30. Kang Y, Stein CS, Heth JA, et al. In vivo gene transfer using a nonprimate lentiviral vector pseudotyped with Ross River virus glycoproteins. *J Virol.* 2002;76:9378-9388.
31. Burns JC, Friedmann T, Driever W, Burrascano M, Yee JK. Vesicular stomatitis virus G glycoprotein pseudotyped retroviral vectors: concentration to very high titer and efficient gene transfer into mammalian and nonmammalian cells. *Proc Natl Acad Sci USA.* 1993;90:8033-8037.
32. Naviaux RK, Costanzi E, Haas M, Verma IM. The pCL vector system: rapid production of helper-free, high-titer, recombinant retroviruses. *J Virol.* 1996;70:5701-5705.
33. Miyoshi H, Blomer U, Takahashi M, Gage FH, Verma IM. Development of a self-inactivating lentivirus vector. *J Virol.* 1998;72:8150-8157.
34. Lois C, Hong EJ, Pease S, Brown EJ, Baltimore D. Germline transmission and tissue-specific expression of transgenes delivered by lentiviral vectors. *Science.* 2002;295:868-872.
35. Hebbard L, Steffen A, Zawadzki V, et al. CD44 expression and regulation during mammary gland development and function. *J Cell Sci.* 2000;113:2619-2630.
36. Miura M, Tamura T, Mikoshiba K. Cell-specific expression of the mouse glial fibrillary acidic protein gene: identification of the cis- and trans-acting promoter elements for astrocyte-specific expression. *J Neurochem.* 1990;55:1180-1188.
37. Brenner M, Kisseberth WC, Su Y, Besnard F, Messing A. GFAP promoter directs astrocyte-specific expression in transgenic mice. *J Neurosci.* 1994;14:1030-1037.
38. Nakamura N, Shida M, Hirayoshi K, Nagata K. Transcriptional regulation of the vimentin-encoding gene in mouse myeloid leukemia M1 cells. *Gene.* 1995;166:281-286.
39. Niwa H, Yamamura K, Miyazaki J. Efficient selection for high-expression transfectants with a novel eukaryotic vector. *Gene.* 1991;108:193-199.
40. Miyazaki J, Takaki S, Araki K, et al. Expression vector system based on the chicken beta-actin promoter directs efficient production of interleukin-5. *Gene.* 1989;79:269-277.
41. Sarthy VP, Brodjian SJ, Dutt K, et al. Establishment and characterization of a retinal Müller cell line. *Invest Ophthalmol Vis Sci.* 1998;39:212-216.
42. Lee D, Geller S, Walsh N, et al. Photoreceptor degeneration in Pro23His and S334ter transgenic rats. *Adv Exp Med Biol.* 2003;533:297-302.
43. Hale IL and Matsumoto B. Resolution of subcellular detail in thick tissue sections: immunohistochemical preparation and fluorescence confocal microscopy. *Methods Cell Biol.* 2002;70:301-335.
44. Mayhew TM, Astle D. Photoreceptor number and outer segment disk membrane surface area in the retina of the rat: stereological data for whole organ and average photoreceptor cell. *J Neurocytol.* 1997;26:53-61.
45. Sastry L, Johnson T, Hobson MJ, Smucker B, Cornetta K. Titering lentiviral vectors: comparison of DNA, RNA and marker expression methods. *Gene Ther.* 2002;9:1155-1162.
46. Newman EA. Current source-density analysis of the b-wave of frog retina. *J Neurophysiol.* 1980;43:1355-1366.
47. Lei B, Perlman I. The contributions of voltage- and time-dependent potassium conductances to the electroretinogram in rabbits. *Vis Neurosci.* 1999;16:743-754.
48. Coil DA, Miller AD. Phosphatidylserine is not the cell surface receptor for vesicular stomatitis virus. *J Virol.* 2004;78:10920-10926.
49. Matlin KS, Reggio H, Helenius A, Simons K. Pathway of vesicular stomatitis virus entry leading to infection. *J Mol Biol.* 1982;156:609-631.
50. Sharkey CM, North CL, Kuhn RJ, Sanders DA. Ross River virus glycoprotein-pseudotyped retroviruses and stable cell lines for their production. *J Virol.* 2001;75:2653-2659.
51. Gauthier R, Joly S, Pernet V, Lachapelle P, Di Polo A. Brain-derived neurotrophic factor gene delivery to Müller glia preserves structure and function of light-damaged photoreceptors. *Invest Ophthalmol Vis Sci.* 2005;46:3383-3392.
52. Isenmann S, Engel S, Kugler S, et al. Intravitreal adenoviral gene transfer evokes an immune response in the retina that is directed against the heterologous lacZ transgene product but does not limit transgene expression. *Brain Res.* 2001;892:229-240.
53. Harvey AR, Kamphuis W, Eggers R, et al. Intravitreal injection of adeno-associated viral vectors results in the transduction of different types of retinal neurons in neonatal and adult rats: a comparison with lentiviral vectors. *Mol Cell Neurosci.* 2002;21:141-157.
54. Chaitin MH and Brun-Zinkernagel AM. Immunolocalization of CD44 in the dystrophic rat retina. *Exp Eye Res.* 1998;67:283-292.
55. Krishnamoorthy R, Agarwal N, Chaitin MH. Upregulation of CD44 expression in the retina during the rds degeneration. *Brain Res Mol Brain Res.* 2000;77:125-130.
56. Cichy J, Pure E. The liberation of CD44. *J Cell Biol.* 2003;161:839-843.
57. Fisher SK, Lewis GP, Linberg KA, Verardo MR. Cellular remodeling in mammalian retina: results from studies of experimental retinal detachment. *Prog Retin Eye Res.* 2005;24:395-431.
58. Kuzmanovic M, Dudley VJ, Sarthy VP. GFAP promoter drives Müller cell-specific expression in transgenic mice. *Invest Ophthalmol Vis Sci.* 2003;44:3606-3613.
59. Gieser L, Swaroop A. Expressed sequence tags and chromosomal localization of cDNA clones from a subtracted retinal pigment epithelium library. *Genomics.* 1992;13:873-876.
60. Lundkvist A, Reichenbach A, Betsholtz C, et al. Under stress, the absence of intermediate filaments from Müller cells in the retina has structural and functional consequences. *J Cell Sci.* 2004;117:3481-3488.
61. Batra RK, Olsen JC, Hoganson DK, Caterson B, Boucher RC. Retroviral gene transfer is inhibited by chondroitin sulfate proteoglycans/glycosaminoglycans in malignant pleural effusions. *J Biol Chem.* 1997;272:11736-11743.
62. Wahlin KJ, Campochiaro PA, Zack DJ, Adler R. Neurotrophic factors cause activation of intracellular signaling pathways in Müller cells and other cells of the inner retina, but not photoreceptors. *Invest Ophthalmol Vis Sci.* 2000;41:927-936.
63. Lau D, McGee LH, Zhou S, et al. Retinal degeneration is slowed in transgenic rats by AAV-mediated delivery of FGF-2. *Invest Ophthalmol Vis Sci.* 2000;41:3622-3633.
64. McGee Sanftner LH, Abel H, Hauswirth WW, Flannery JG. Glial cell line derived neurotrophic factor delays photoreceptor degeneration in a transgenic rat model of retinitis pigmentosa. *Mol Ther.* 2001;4:622-629.
65. Weise J, Isenmann S, Klocker N, et al. Adenovirus-mediated expression of ciliary neurotrophic factor (CNTF) rescues axotomized rat retinal ganglion cells but does not support axonal regeneration in vivo. *Neurobiol Dis.* 2000;7:212-223.
66. Lewis GP, Fisher SK. Up-regulation of glial fibrillary acidic protein in response to retinal injury: its potential role in glial remodeling and a comparison to vimentin expression. *Int Rev Cytol.* 2003;230:263-290.